SUPPLEMENTARY INFORMATION

List of Tables:

List of Figures:

Model #		A					B				C	
Group		G1a-f	G1'a-f		G2a-f	G3a-f	G1a-f	G1'a-f	G2a-f	G3a-f	a-f	
a/d ratio		0.1			0.05	0.5	0.1		0.05	0.5	< 0.2	
Source radius a [m]		50	500		50	500	50	500	50	500	500	
Source 1 depth-to-centre [m]		500	5000		1000	1000	500	5000	1000	1000	2750-5000	
Source separation	[m]	125-500	1250-5000		125-500	1250-5000	125-500	1250-5000	125-500	1250-5000	750-4500	
	[radii]	2.5(a), 3(b), 4(c), 5(d), 8(e), 10(f)									1.5(a), 2(b), 3(c), 4(d), 7(e), 9(f)	
Source 1 / Source 2 pressurization or opening		20 MPa / 20 MPa; 20 MPa / -20 MPa; 200 MPa / 200 MPa (G1a-f only)					20 MPa / 20 MPa; 20 MPa / -20 MPa				20 MPa / 1 m; -20 MPa / 1 m	
Domain dimensions[1] [km]		20× 20× 10	200×200×100		20× 20× 10	200×200×100	20× 20× 10	40× 40× 15	20× 20× 10	20× 20× 10	$50^{(*)} \times 50^{(*)} \times 60$	
Mesh statistics	Tetrahedra	25826	50326	58774	24316	36264	26893	14594	26893	37268	22122	
	Elements[2]	113235	130567	169352	104396	158606	107029	84956	107029	152452	86129	
	A.E.Q [3]	0.66	0.88	0.89	0.66	0.68	0.60	0.78	0.60	0.67	0.71	
Benchmarking [%]	Source (M/O)	M(a-f)	M1+M2	M(a-f)	M(a-f)	M(a-f)	M(a-f)	M(a-f)	M(a-f)	M(a-f)	M(f)	O(a-f)
	ε_x	0.4	0.6	0.6	0.4	0.9	0.6	3.0	0.6	3.0	0.6	0.3
	ε_y	0.3	0.6	0.6	0.3	0.5	0.3	1.5	0.3	1.4	0.5	0.5
	ε_z	1.3	1.9	0.6	1.3	1.4	1.2	1.5	1.2	3.1	1.5	1.3
	$\Xi_x\|_{min}$	0.2	0.1	0.0	0.2	0.5	0.4	2.9	0.4	0.9	0.0	4.3
	$\Xi_x\|_{max}$	0.3	0.0	0.0	0.3	0.5	0.5	2.9	0.5	0.9	0.5	0.1
	$\Xi_z\|_{min}$	n/a	n/a	n/a	n/a	n/a	n/a	n/a	n/a	n/a	n/a	0.1
	$\Xi_z\|_{max}$	0.6	0.2	0.2	0.6	1.2	1.4	0.2	1.4	1.8	0.6	0.0

Table A-1: Models A-D source parameters, models statistics, and benchmarking. On this page are presented parameters and results for Models A-C.
Continued on Next Page…

Model #		DI							DII					
Group		a-f							a-f					
a/d ratio		0.2							0.2					
Source radius a [m]		500							500					
Source 1 depth-to-centre [m]		2500							2500					
Source separation	[m]	750-4500							1250-5000					
	[radii]	1.5(a), 2(b), 3(c), 4(d), 7(e), 9(f)							1.5(a), 2(b), 3(c), 4(d), 7(e), 9(f)					
Source 1 / Source 2 pressurization or opening		20 MPa / 1 m (M1, 2); 20 MPa / 12 MPa (M3); -20 MPa / 1 m (M1, 2); -20 MPa / 12 MPa (M3)							20 MPa / 1 m; -20 MPa / 1 m					
Domain dimensions [1] [km]		110× 100× 35							120× 50 [*] × 50					
Mesh statistics	Tetrahedra Elements [2]	50665							21876					
	A.E.Q [3]	184356							67078					
		0.63							0.66					
Benchmarking [%]	Source (M/O)	M+0 (DIa)	M(DIa)	M(DIf)	M(DIIf)	O (d_T =0.2 km)			O (d_T =1 km)			O (d_T =2 km)		
	Method	M1	n/a	n/a	n/a	M1	M2	M3	M1	M2	M3	M1	M2	M3
	ε_x	2.3	2.8	0.6	0.4	3.0	2.9	5.0	4.0	2.5	0.8	2.6	2.0	0.6
	ε_y	2.7	0.6	0.9	0.8	3.0	3.1	10.0	3.0	2.9	1.3	2.6	2.6	0.8
	ε_z	2.0	2.9	1.7	0.9	2.0	2.3	10.0	2.0	2.3	1.9	2.8	2.8	3.4
	$\Xi_x\|_{min}$	4.9	2.7	0.4	0.4	4.0	3.7	1.0	5.0	2.4	0.4	1.0	2.2	0.4
	$\Xi_x\|_{max}$	0.5	2.1	0.3	0.3	4.0	3.5	1.0	0.3	2.6	0.8	3.3	2.1	0.3
	$\Xi_z\|_{min}$	2.0	n/a	n/a	n/a	2.0	2.1	10.0	2.5	2.6	0.0	3.5	3.5	1.0
	$\Xi_z\|_{max}$	n/a	1.1	0.3	0.4	3.0	2.8	7.0	2.3	2.1	0.2	1.2	1.2	1.0

Table A-1: *(Continued)* Models A-D: Description of the geometry and physical parameters of the combined models; Models statistics; Benchmarking of the various models individual spherical sources (M) and dike (0) modelled with Methods 1-3 against either Mogi (1958) and Okada (1992) solution. In all models, the medium elastic parameters are $\nu = 0.25$ and $E = 10$ GPa. The dike width and length are both 1 km. For Models DI and DII (juxtaposed and aligned spherical source and dike), the dike model benchmarked are located at a depth-to-top d_T. The 'M1+M2' (A) and 'M+0 (DIa)' columns correspond to the comparison between the sum of the two analytical sources against the sum of the two FEM sources displacement solutions. [1]Domain dimensions correspond to Width×Length×Height,[*] mark dimensions for which axisymmetry has been used to reduce computing time; [2]Elements are tetrahedral; [3]'A.E.Q' is the average elements quality.

Model	$\Delta P_1 = \Delta P_2 = 20$ MPa					$\Delta P_1 = \Delta P_2 = 200$ MPa					$\Delta P_1 = -\Delta P_2 = 20$ MPa				
	ϵ_x	ϵ_y	ϵ_z	Ξ_x	Ξ_z	ϵ_x	ϵ_y	ϵ_z	Ξ_x	Ξ_z	ϵ_x	ϵ_y	ϵ_z	Ξ_x	Ξ_z
G1a	3.3	3.3	5.6	7.0	13.9	3.3	3.3	5.6	7.0	13.9	6.5	5.6	11.4	7.2	13.6
G1b	2.2	2.2	4.1	4.6	8.9	2.2	2.2	4.1	4.6	8.9	3.9	3.9	7	4.6	8.4
G1c	1.1	1.1	2.4	2.2	4.2	1.1	1.1	2.4	2.2	4.2	1.7	1.7	3.2	2.1	3.9
G1d	0.7	0.7	1.7	1.1	2.3	0.7	0.7	1.7	1.1	2.3	0.9	0.9	1.8	1.1	2.1
G1e	0.4	0.4	1.2	0.3	0.7	0.4	0.4	1.2	0.3	0.7	0.3	0.3	0.6	0.3	0.6
G1f	0.4	0.4	1.1	0.2	0.5	0.4	0.4	1.1	0.2	0.5	0.2	0.2	0.4	0.2	0.3
G1'a	3.3	3.3	5.9	7.0	13.7	–	–	–	–	–	6.9	6.9	11.3	7.6	14.3
G1'b	2.2	2.2	4.4	4.6	8.7	–	–	–	–	–	4.2	4.1	6.9	4.0	9.0
G1'c	1.2	1.2	2.8	2.1	4.1	–	–	–	–	–	1.9	1.9	3.3	2.0	3.7
G1'd	1.0	1.0	2.2	1.1	2.3	–	–	–	–	–	1.1	1.1	1.9	1.1	1.9
G1'e	0.7	0.7	1.6	0.2	0.6	–	–	–	–	–	0.6	0.6	1.0	0.3	0.5
G1'f	0.7	0.7	1.5	0.1	0.2	–	–	–	–	–	0.5	0.5	0.9	0.1	0.4
G2a	7	7	9.4	7.2	14.7	–	–	–	–	–	4.6	4.6	8.1	7.4	13.7
G2b	4.8	4.8	6.6	4.9	9.7	–	–	–	–	–	2.8	2.8	5	4.5	8.3
G2c	2.6	2.6	3.8	2.5	4.8	–	–	–	–	–	1.3	1.3	2.3	2	3.7
G2d	1.7	1.7	2.7	1.4	2.9	–	–	–	–	–	0.7	0.7	1.3	1	1.9
G2e	1	0.9	1.8	0.5	1.3	–	–	–	–	–	0.2	0.2	0.5	0.2	0.3
G2f	0.9	0.9	1.6	0.4	1.1	–	–	–	–	–	0.2	0.2	0.5	0.1	0
G3a	3.9	3.7	7.6	4.8	6.9	–	–	–	–	–	4.3	4.2	8.9	4.7	9.7
G3b	3.1	2.9	5.7	2.8	3.8	–	–	–	–	–	2.7	2.6	5.8	2.9	6.7
G3c	2.4	2.1	3.7	1.1	0.9	–	–	–	–	–	1.5	1.4	3.6	1.4	4
G3d	2.1	1.8	2.9	0.5	0.3	–	–	–	–	–	1.2	1.1	3.2	0.9	2.9
G3e	2.0	1.7	1.9	0.0	1.4	–	–	–	–	–	1.2	1.1	3.8	0.4	1.7
G3f	1.9	1.6	1.4	0.1	1.6	–	–	–	–	–	1.4	1.2	4.4	0.3	1.4

Table A-2. Model A, Groups 1-3: Surface (ϵ) and maximum local (Ξ) discrepancies [%] obtained for $\Delta P_1 = \Delta P_2 = 20$ MPa, $\Delta P_1 = -\Delta P_2 = 20$ MPa (Groups G1-3), and $\Delta P_1 = \Delta P_2 = 200$ MPa (Group G1). Depending on the model, $\Xi_z = \Xi_z\Big|_{\max}$ or $\Xi_z\Big|_{\min}$, and similarly for Ξ_x. Elastic parameters are $\nu = 0.25$ and $E = 10$ GPa. See also Figure 4.

Model	$\Delta P_1 = \Delta P_2 = 20$ MPa					$\Delta P_1 = -\Delta P_2 = 20$ MPa				
	ϵ_x	ϵ_y	ϵ_z	Ξ_x	Ξ_z	ϵ_x	ϵ_y	ϵ_z	Ξ_x	Ξ_z
G1a	6.0	5.3	4.9	0.6	7.9	7.4	9.7	8.9	7.1	13.5
G1b	6.4	5.6	5.3	1.4	9.0	4.4	5.6	5.4	4.2	8.4
G1c	2.1	1.6	1.8	0.1	1.9	1.9	2.6	2.4	1.8	3.7
G1d	1.3	0.9	1.3	0.3	0.9	1.0	1.5	1.4	0.9	2.0
G1e	0.8	0.4	1.2	0.2	0.0	0.3	0.5	0.4	0.2	0.5
G1f	0.7	0.4	1.2	0.2	0.1	0.2	0.4	0.4	0.2	0.0
G1'a	5.3	5.8	4.6	1.4	6.3	9.6	13.1	12.3	8.9	13.8
G1'b	4.5	4.7	3.8	1.1	3.5	6.0	8.2	10.0	6.0	9.1
G1'c	3.3	2.6	2.8	1.9	0.8	3.5	5.2	4.6	3.0	4.8
G1'd	3.3	2.1	3.2	1.9	0.2	1.4	1.8	2.0	1.5	2.9
G1'e	3.3	1.5	3.4	2	1.7	0.8	1.4	1.3	0.7	1.1
G1'f	4	2.0	3.4	3.0	2.0	0.7	1.2	1.0	0.6	0.7
G2a	4.8	5.5	4.7	0.5	7.2	8.1	10.9	10.0	7.5	14.0
G2b	3.3	3.5	3.0	0.3	4.0	5.0	6.2	6.0	4.0	8.6
G2c	1.9	1.8	1.8	0.3	1.4	2.1	3.3	2.8	1.8	4.1
G2d	1.3	1.2	1.5	1.3	0.3	1.2	1.8	1.7	0.9	1.3
G2e	1.0	0.7	1.7	0.4	0.7	0.5	0.7	0.7	0.4	0.7
G2f	1.0	0.7	1.7	0.5	0.6	0.3	0.6	0.5	0.2	0.1
G3a	6.7	5.9	6.7	2.1	9.8	5.7	8.0	6.8	7.3	7.1
G3b	5.4	3.6	4.8	1.9	5.0	2.9	4.0	3.4	3.1	2.5
G3c	4.5	1.6	3.7	1.2	2.0	1.0	1.9	1.2	0.0	0.9
G3d	4.1	1.4	3.9	0.9	1.4	0.9	1.2	1.0	0.8	0.9
G3e	3.7	1.6	4.1	0.8	1.2	1.2	0.8	1.0	0.9	1.9
G3f	3.7	1.7	4.2	1.0	1.3	1.2	0.7	1.0	0.9	1.9

Table A-3. Model B, Groups 1-3: Surface (ϵ) and maximum local (Ξ) discrepancies [%] obtained for $\Delta P_1 = \Delta P_2 = 20$ MPa. Elastic parameters are $\nu = 0.25$ and $E = 10$ GPa. See also Figure 5.

Model		ϵ (%)			Ξ (%)			
		ϵ_x	ϵ_y	ϵ_z	$\Xi_x\big\vert_{\min}$	$\Xi_x\big\vert_{\max}$	$\Xi_z\big\vert_{\min}$	$\Xi_z\big\vert_{\max}$
ΔP=20 MPa	Ca	1.3	1.2	1.6	n/a	1.2	n/a	1.5
	Cb	0.7	1.0	1.3	n/a	0.8	n/a	1.1
	Cc	0.4	0.6	0.9	n/a	0.4	n/a	0.4
	Cd	0.2	0.6	1.0	n/a	0.1	n/a	0.1
	Ce	0.2	0.5	1.3	n/a	0.2	n/a	0.2
	Cf	0.3	0.5	1.4	n/a	0.01	n/a	0.3
ΔP=-20 MPa	Ca	9.0	0.4	1.9	2.4	4.0	1.0	n/a
	Cb	4.0	0.4	1.6	1.7	1.9	0.8	n/a
	Cc	1.3	0.4	1.3	1.3	0.8	0.4	n/a
	Cd	0.3	0.4	1.1	2.2	0.1	0.4	3.8
	Ce	0.2	0.4	0.9	4.1	0.2	0.5	0.3
	Cf	0.2	0.5	0.9	3.0	0.1	0.2	0.1
ΔP=20 MPa	DIIa	0.3	0.7	1.5	0.2	0.1	n/a	0.7
	DIIb	0.4	0.7	1.3	0.2	0.4	n/a	0.3
	DIIc	0.4	0.7	1.2	0.3	0.5	n/a	0.1
	DIId	0.4	0.7	1.2	0.3	0.3	n/a	0.1
	DIIe	0.4	0.9	1.3	0.3	0.3	n/a	0.4
	DIIf	0.5	1.0	0.7	0.3	0.4	0.5	n/a
ΔP=-20 MPa	DIIa	0.9	1.4	1.4	0.7	0.6	1.7	n/a
	DIIb	0.8	1.1	1.1	0.5	0.3	1.3	n/a
	DIIc	0.7	0.9	0.9	0.6	0.2	0.9	n/a
	DIId	0.5	0.7	0.8	0.4	0.3	0.6	n/a
	DIIe	0.5	0.9	0.8	0.4	0.6	0.7	n/a
	DIIf	0.4	1.0	1.2	0.3	0.3	n/a	0.3

Table A-4. Model C and D2: Surface (ϵ) and maximum local (Ξ) discrepancies obtained for an dike opening by 1 m superposed (Model C) or horizontaly aligned (Model DII, see Figure 2) to either an inflating ($\Delta P = 20$ MPa) or a deflating spherical source ($\Delta P = -20$ MPa). Elastic parameters are $\nu = 0.25$ and $E = 10$ GPa.

Model			ϵ (%)			Ξ (%)			
			ϵ_x	ϵ_y	ϵ_z	$\Xi_x\big\|_{\min}$	$\Xi_x\big\|_{\max}$	$\Xi_z\big\|_{\min}$	$\Xi_z\big\|_{\max}$
Model DI,dike op. 1 m	ΔP=20 MPa	DIa	97.2	12.3	12.6	82.3	57.5	n/a	15.1
		DIb	87.7	9.6	9.0	61.4	42.6	n/a	11.5
		DIc	45.8	4.2	6.1	42.3	27.0	n/a	6.9
		DId	28.3	2.3	4.1	26.5	16.0	n/a	4.1
		DIe	12.0	1.8	2.2	13.0	6.1	n/a	1.5
		DIf	8.7	2.2	2.4	8.4	3.9	n/a	0.6
	ΔP=-20 MPa	DIa	553.7	9.8	22.5	298.8	185.1	5.3	n/a
		DIb	382.5	10.1	12.6	200.2	65.8	3.6	n/a
		DIc	148.0	3.4	6.6	86.5	54.3	2.6	468.6
		DId	74.5	2.2	4.1	43.1	31.6	1.5	83.9
		DIe	19.8	1.2	2.0	9.2	7.1	0.4	16.5
		DIf	12.0	1.1	1.9	5.1	3.7	0.3	12.1
Model DI,rel. dike op. 1 m	ΔP=20 MPa	DIa	7.1	7.6	5.7	5.9	2.7	n/a	7.2
		DIb	4.5	5.4	4.2	4.1	0.8	n/a	5.7
		DIc	1.8	2.0	2.4	1.8	0.7	n/a	3.4
		DId	0.8	0.7	1.8	0.2	1.1	n/a	2.2
		DIe	0.8	1.2	1.4	0.3	1.0	n/a	1.1
		DIf	0.8	1.8	1.9	1.0	0.9	n/a	0.5
	ΔP=-20 MPa	DIa	24.1	7.6	6.8	8.7	0.5	7.0	n/a
		DIb	13.3	5.0	4.2	4.4	0.6	5.1	n/a
		DIc	3.6	1.9	1.6	1.0	0.9	2.9	n/a
		DId	1.3	1.0	1.3	0.4	0.7	1.6	n/a
		DIe	1.6	0.7	1.0	0.8	1.0	0.1	6.4
		DIf	1.3	0.8	1.4	0.2	0.9	0.1	6.0
Model DI, crack 12 MPa	ΔP=20 MPa	DIa	14.3	12.3	9.1	11.2	9.3	n/a	5.5
		DIb	9.2	6.9	6.6	8.6	5.9	n/a	4.2
		DIc	3.9	3.0	3.1	4.8	1.9	n/a	2.4
		DId	2.0	1.3	2.0	0.2	0.6	n/a	1.5
		DIe	1.0	0.7	1.5	0.2	0.0	n/a	0.8
		DIf	1.1	1.2	2.2	1.6	0.1	n/a	0.3
	ΔP=-20 MPa	DIa	11.1	15.5	11.9	17.6	2.7	12.9	n/a
		DIb	5.6	6.0	5.7	5.5	0.2	6.9	n/a
		DIc	2.8	1.9	2.0	0.4	0.9	3.2	n/a
		DId	1.5	1.0	1.2	0.5	0.7	1.5	n/a
		DIe	0.6	0.6	0.6	0.7	0.2	0.2	0.9
		DIf	0.5	0.9	1.0	0.7	0.1	0.2	1.6

Table A-5. Model DI, Methods 1-3: Discrepancies obtained for a spherical source pressurized by $\Delta P = 20$ MPa or $\Delta P = -20$ MPa and a dike opening by 1 m modelled applying on its walls either a fixed displacements (Method 1), relative displacements (Method 2), or an overpressure of 12 MPa (Method 3). Elastic parameters are $\nu = 0.25$ and $E = 10$ GPa. See also corresponding Figures 8 & A-1

		Model A-G1'a	Model DIa Method 1	Model DIa Method 2	Model DIa Method 3
Mogi source 1	$\Delta P1$ [MPa]	16-18	(-21)-(-19)	(-21)-(-18)	(-22)-(-18)
	misfit to ref. model [MPa]	(-2)-(-4)	up to ± 1	(-1)-(+2)	up to ± 2
	misfit to ref. model [%]	(-10)-(-20)	up to ± 5	(-5)-(+10)	up to ± 10
Mogi source 2	$\Delta P2$ [MPa]	13-16	n/a	n/a	n/a
	misfit to ref. model [MPa]	(-4)-(-7)	n/a	n/a	n/a
	misfit to ref. model [%]	(-20)-(-35)	n/a	n/a	n/a
Okada source	Opening [m]	n/a	0.5-1	0.8	0.8-1.2
	misfit to ref. model [m]	n/a	0-(-0.5)	(-0.2)	up to ± 0.2
	misfit to ref. model [%]	n/a	0-(-50)	(-20)	up to ± 20
Source separation [radii]		4.2-5.1	1.5-2.2	1.5-1.6	1.3-1.9
Misfit to reference model [radii]		(+1.7)-(+2.6)	$\leq +0.7$	$\leq +0.1$	(+0.1)-(+0.4)
Misfit to reference model [%]		(+20)-(+30)	$\leq +45$	$\leq +7$	(+7)-(+27)
Discrepancies [%]	mean(ϵ)		≥ 150	$\leq 5-10$	$10-20$
	ϵ_x	< 5	≥ 150	$6-40$	$6-15$
	ϵ_y	$\lesssim 5$	$6-10$	$\leq 5-10$	$15-20$
	ϵ_z	< 5	$20-25$	$\leq 5-10$	$\leq 5-15$
	$\Xi_x\|_{\min}$	< 5	≥ 150	$\leq 5-30$	$\leq 5-10$
	$\Xi_x\|_{\max}$	< 5	≥ 150	$\leq 5-8$	$\leq 5-6$
	$\Xi_z\|_{\min}$	< 5 n/a	$\leq 5-10$	$\leq 5-10$	$\leq 5-15$
	$\Xi_z\|_{\max}$	< 5	n/a	n/a	n/a

Table A-6. Summary of source parameters estimated from minimum discrepancies for Model A-G1'a and for Model DIa using respectively Figure 12 or Figure 15 and in Figures 13 & 14. The source parameters range are primarily estimated looking at the minimum mean(ϵ) value, secondly at the minimum of all surface (ϵ) and maximum local (Ξ) discrepancies, simultaneously.

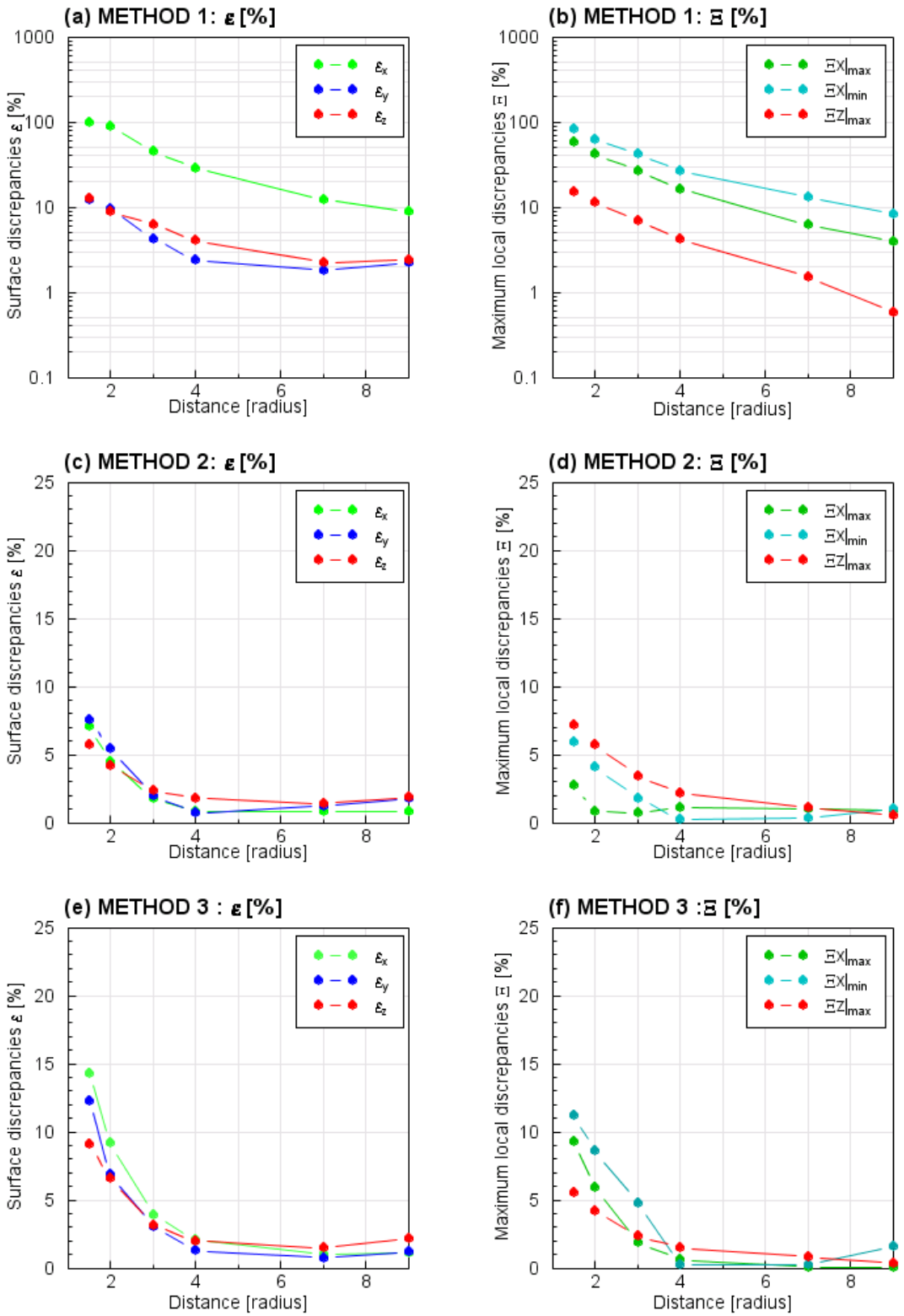

Figure A-1. Model DI: Surface (ϵ) and maximum local (Ξ) discrepancies *vs* source separation, obtained for models combining a spherical source pressurized by $\Delta P = +20$ MPa juxtaposed to a dike opening by 1 m, modelled with Methods 1-3 (*from top to bottom*). Corresponding discrepancies values are listed in Table A-4.

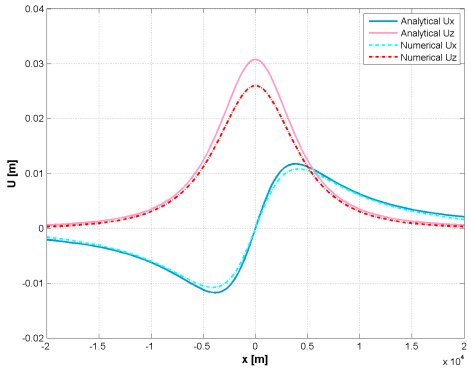

(a) Model A, $\Delta P2 = 20$ MPa, Distance 2.5 (G'1a)

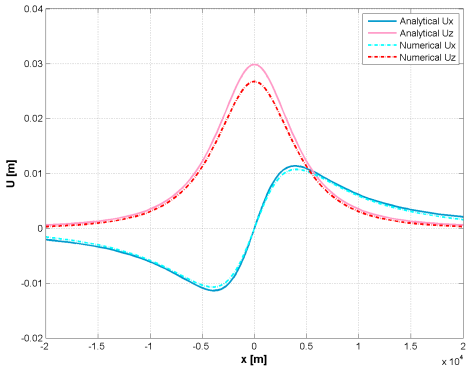

(b) Model A, $\Delta P2 = 20$ MPa, Distance 3 (G'1b)

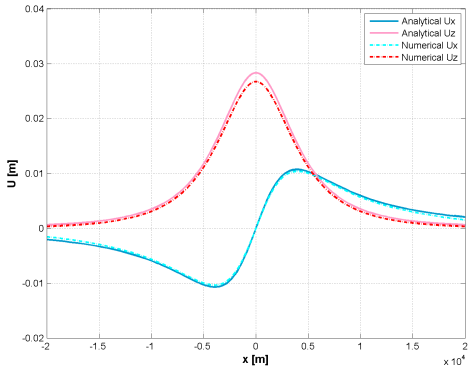

(c) Model A, $\Delta P2 = 20$ MPa, Distance 4 (G'1c)

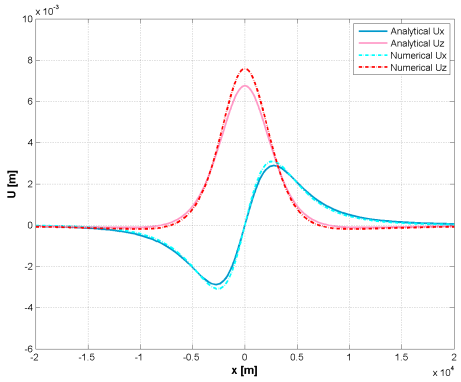

(d) Model A, $\Delta P2 = -20$ MPa, Distance 2.5 (G'1a)

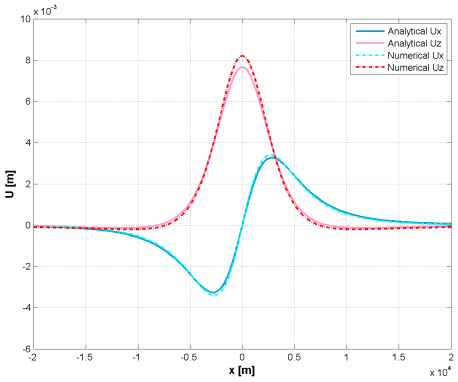

(e) Model A, $\Delta P2 = -20$ MPa, Distance 3 (G'1b)

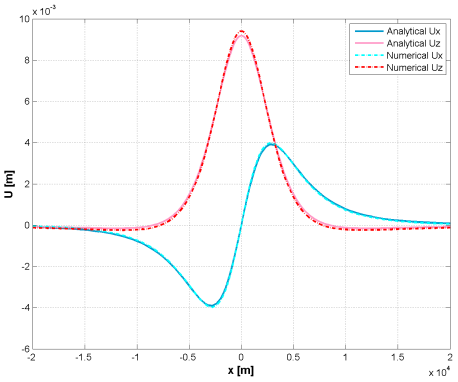

(f) Model A, $\Delta P2 = -20$ MPa, Distance 4 (G'1c)

Figure A-2: Models A (Group G1'a): Surface displacements across the centre of the deformation sources for models with two superposed sources separated by a distance of 2.5, 3 and 4 radii. The upper source pressurization is $\Delta P1 = 20$ MPa (*top*) and the lower source pressurization is $\Delta P2 = \pm 20$ MPa (*bottom*).

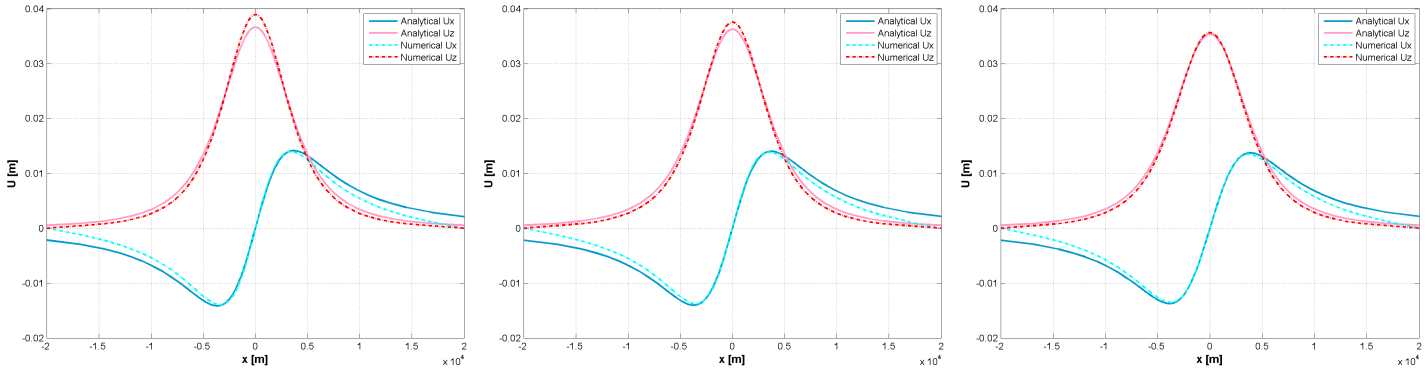

(a) Model B, $\Delta P2 = 20$ MPa, Distance 2.5 (G'1a)

(b) Model B, $\Delta P2 = 20$ MPa, Distance 3 (G'1b)

(c) Model B, $\Delta P2 = 20$ MPa, Distance 4 (G'1c)

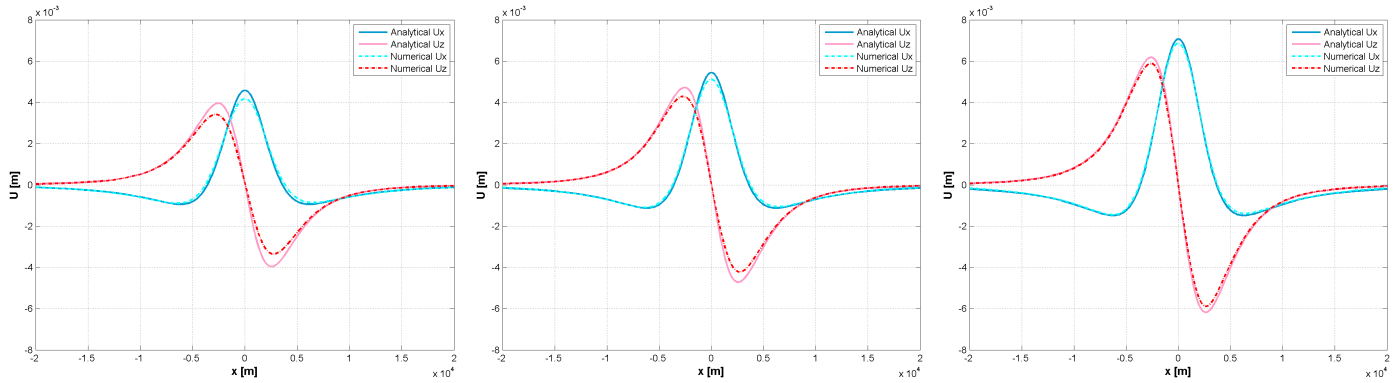

(d) Model B, $\Delta P2 = -20$ MPa, Distance 2.5 (G'1a)

(e) Model B, $\Delta P2 = -20$ MPa, Distance 3 (G'1b)

(f) Model B, $\Delta P2 = -20$ MPa, Distance 4 (G'1c)

Figure A-3: Models B (Group G1'a): Surface displacements across the centre of the deformation sources for models with two superposed sources separated by a distance of 2.5, 3 and 4 radii. The left-hand source pressurization is $\Delta P1 = 20$ MPa (*top*) and the right-hand source pressurization is $\Delta P2 = \pm 20$ MPa (*bottom*).

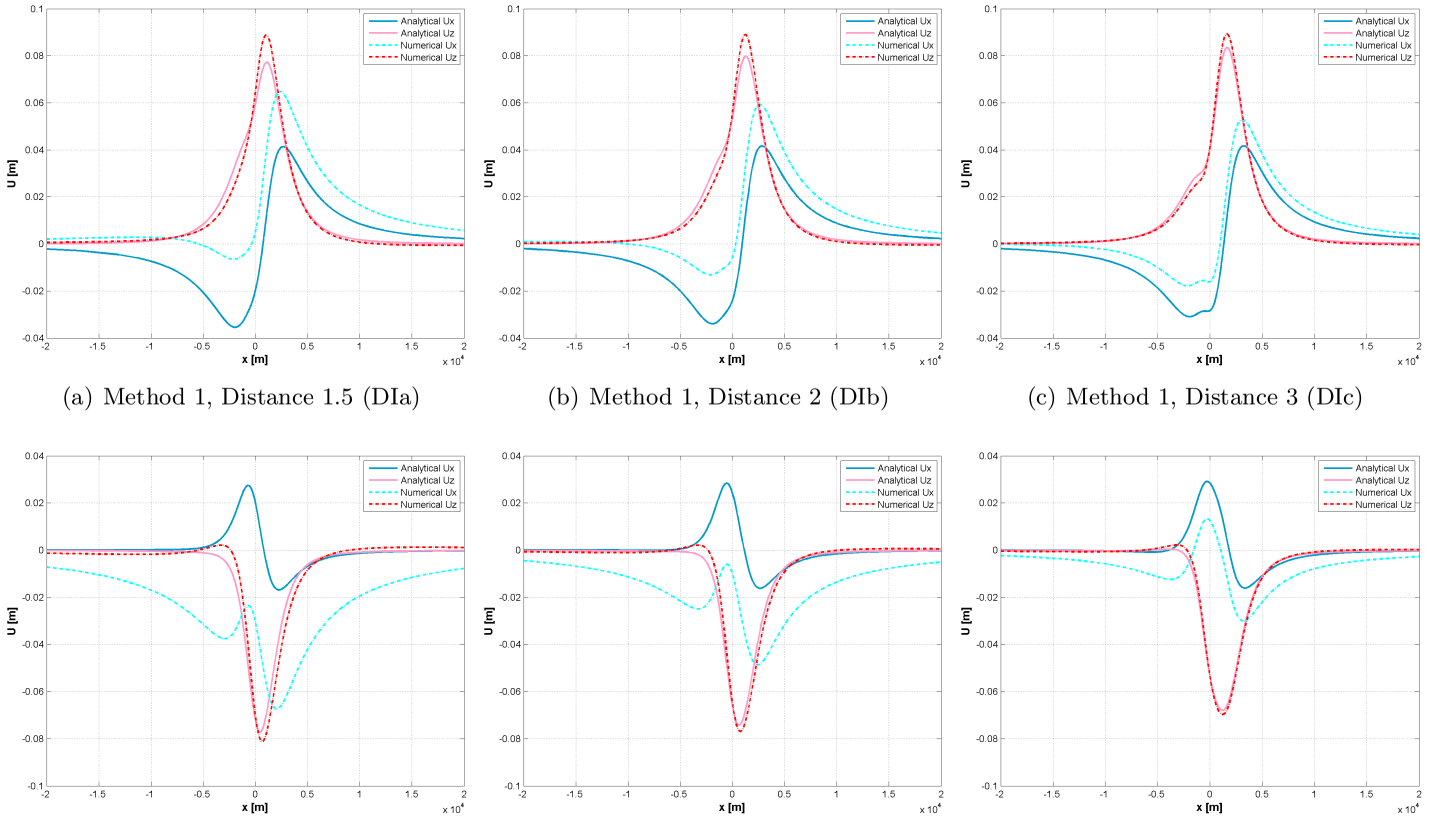

(a) Method 1, Distance 1.5 (DIa) (b) Method 1, Distance 2 (DIb) (c) Method 1, Distance 3 (DIc)

(d) Method 1, Distance 1.5 (DIa) (e) Method 1, Distance 2 (DIb) (f) Method 1, Distance 3 (DIc)

Figure A-4: Model DIa,b,c (Method 1): Surface displacements across the centre of the deformation sources for models of a dike opening by 1 m, modelled by Method 1, juxtaposed to a spherical source pressurized by either $\Delta P2 = +20$ MPa (*top*) or $\Delta P2 = -20$ MPa (*bottom*). The sources are separated by a distance of 1.5 radii, 2 and 3 radii.

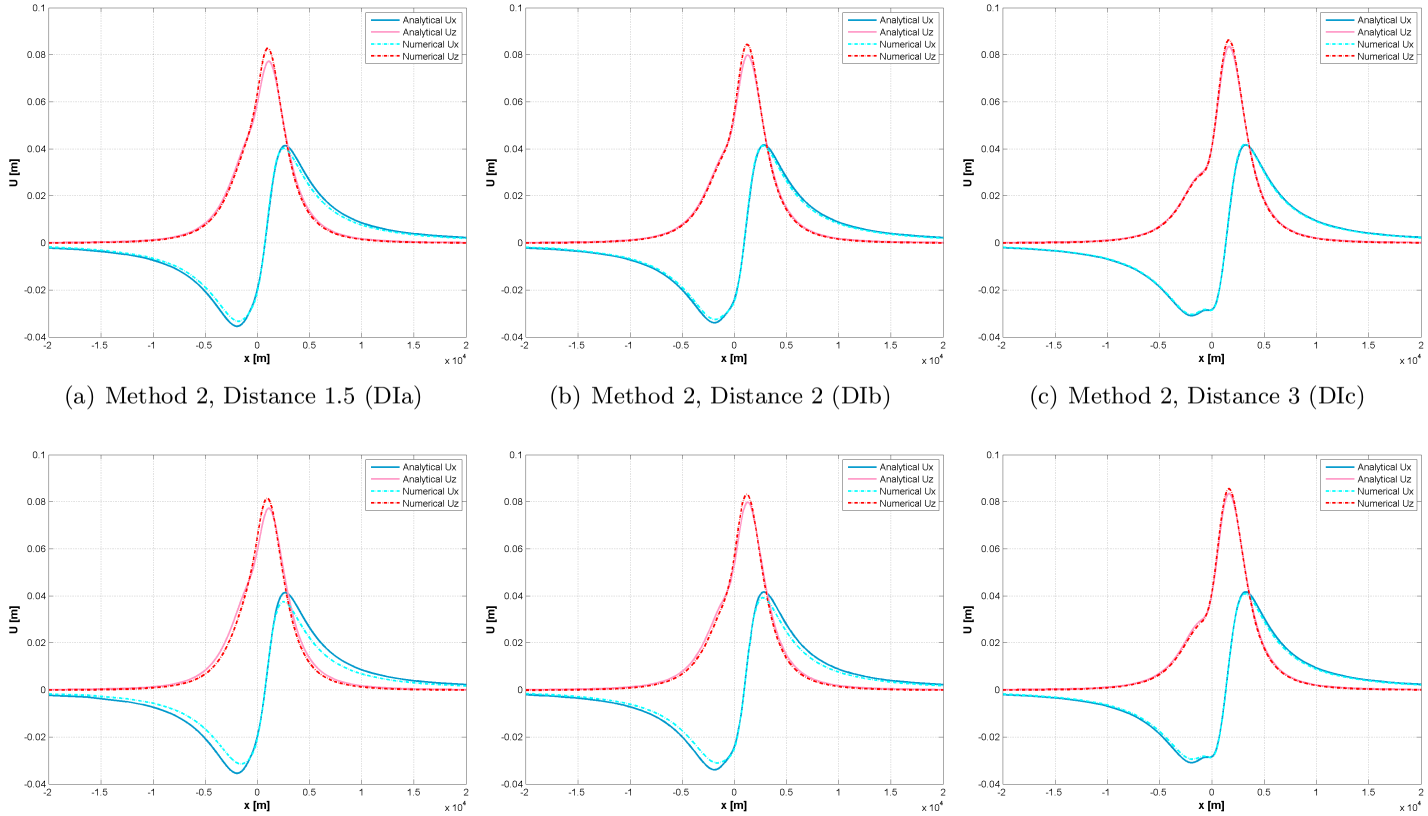

(a) Method 2, Distance 1.5 (DIa) (b) Method 2, Distance 2 (DIb) (c) Method 2, Distance 3 (DIc)

(d) Method 3, Distance 1.5 (DIa) (e) Method 3, Distance 2 (DIb) (f) Method 3, Distance 3 (DIc)

Figure A-5: Model DIa,b,c: Surface displacements across the centre of the deformation sources for models of a dike opening by 1 m, modelled by Method 2 (*top row*) or Method 3 (*bottom row*), juxtaposed to a spherical source pressurized by $\Delta P2 = +20$ MPa. The sources are separated by a distance of 1.5 radii, 2 and 3 radii.

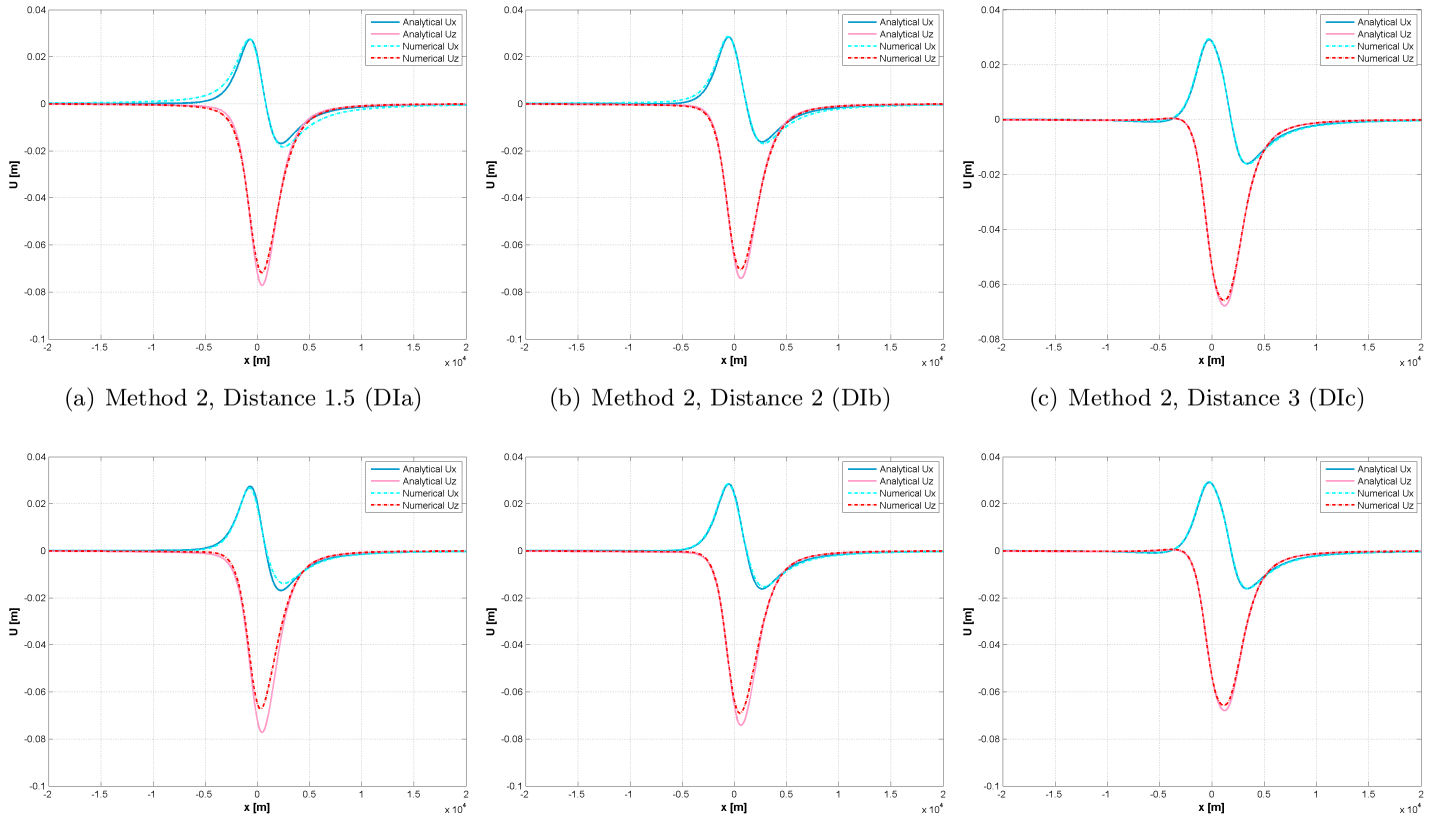

(a) Method 2, Distance 1.5 (DIa)

(b) Method 2, Distance 2 (DIb)

(c) Method 2, Distance 3 (DIc)

(d) Method 3, Distance 1.5 (DIa)

(e) Method 3, Distance 2 (DIb)

(f) Method 3, Distance 3 (DIc)

Figure A-6: Model DIa,b,c: Surface displacements across the centre of the deformation sources for models of a dike opening by 1 m, modelled by Method 2 (*top row*) or Method 3 (*bottom row*), juxtaposed to a spherical source pressurized by $\Delta P2 = -20$ MPa. The sources are separated by a distance of 1.5 radii, 2 and 3 radii.

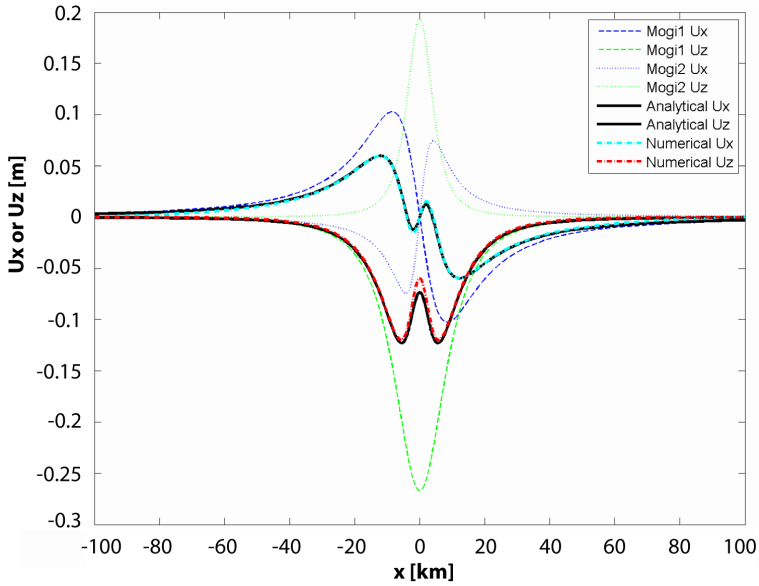

(a) Model CS1: Displacements profiles (m)

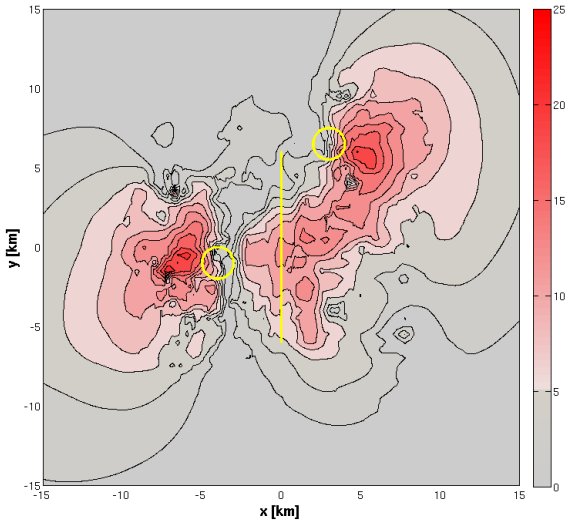

(b) Model CS3: discrepancies in U_x (%)

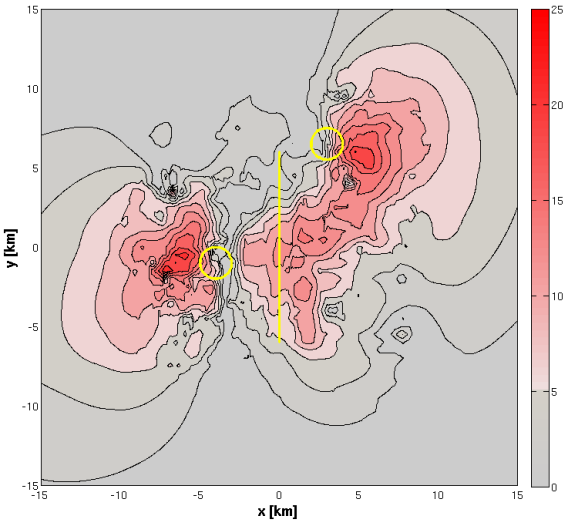

(c) Model CS3: discrepancies in U_z (%)

Figure A-7. Model CS1 and CS3 (adapted from Elsworth et al., 2008 and Wright et al., 2006 for SHV, Montserrat, West Indies and the Dabbahu segment, Afar, Ethiopia, respectively). *Top: Model CS1.* Profiles of the analytical and numerical solutions for the two sources individually and combined. *Bottom: Model CS3.* Contourmaps of the horizontal (**b**) and vertical (**c**) discrepancies [%] between analytical and FE solutions, normalized by $U_z^{An}\Big|_{\max}$ $U_z^{An}\Big|_{\max}$, respectively. Projection of the source position onto the surface is indicated in yellow. Negligible discrepancies ($< 5\%$) are mapped in grey. Corresponding geometry, physical parameters and discrepancies values are listed in Table 3.

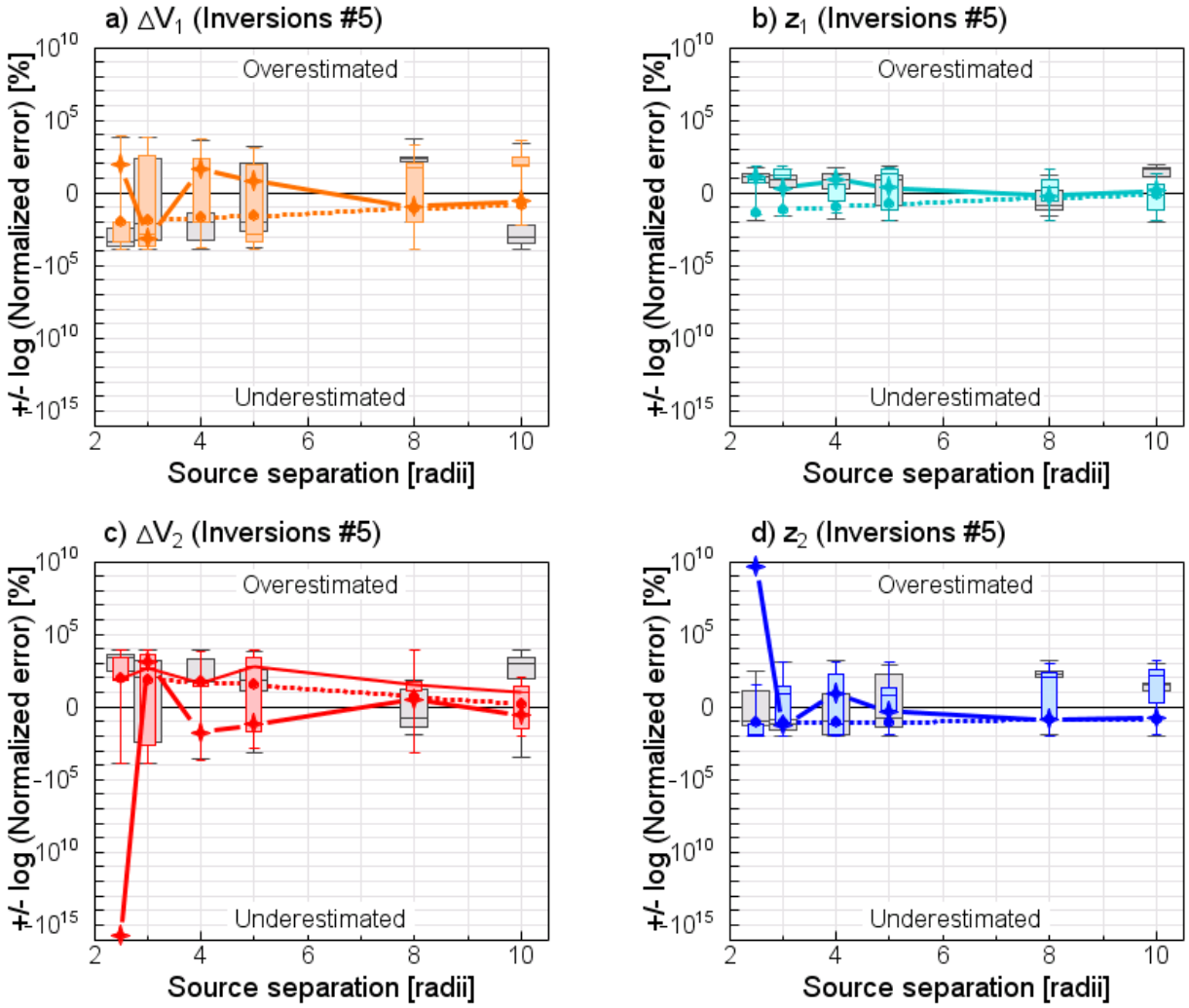

Figure A-8. Inversions #5: errors between original and retrieved parameters values obtained for a population of 100 inversions of the solution of the synthetic datasets (numerical reference model), using combined analytical models corresponding to Model A-G1'a to f. The reference models consist of two superposed spherical sources of radius a=500 m pressurized by $\Delta P1 = \Delta P2 = 20$ MPa. A Gaussian noise with standard deviation 1 cm has been added to the synthetic solution, which has then been bootstrapped. The population of error between reference and retrieved parameter normalized by the reference parameter is plotted against the reference model source separation. The error distribution obtained for the full FE model and for the 'M1+M2' summed model are indicated in coloured and grey, respectively. The box-and-whiskers plot indicate the minimum, the first quartile, the median, the third quartile and the maximum of the error population. The error obtained for the original synthetic dataset are indicated with a solid line for the full FE model and with a dotted line for the 'M1+M2' summed model. The sources are separated by a distance of 2.5, 3, 4, 5, 8, 9 radii. Inversions #5 retrieve all parameters, source volume changes and depths: (a) the deeper source volume change ΔV_2 and (b) depth Δz_2, and (c) the shallower source volume change ΔV_1 and (d) depth z_1.